A CYCLONIC-STATIC MICRO BUBBLE FLOTATION COLUMN FOR ENHANCING COALESCENCE OF OIL DROPLETS FROM EMULSION

Xiaobing LI, Xiaokang YAN, Haijun ZHANG

National Center for Coal Preparation and Purification Engineering Research, China University of Mining and Technology, Xuzhou, Jiangsu, PR China, Xiaobing.li@cumt.edu.cn

Abstract: In this work a novel cyclonic-static micro bubble flotation column, using hydraulic separator with a conventional flotation column, was developed to separate oil droplets from emulsions. The system integrated the cyclonic and laminar flow coalescence with the pipe flow coalescence. The effect of process parameters such as circulation pressure, aeration rate, feed volumetric flow rate and viscosity of fluid on the efficiency of multi-flow pattern coalescence was investigated. The obtained results indicated that the coalescence efficiency increased with the circulation pressure, feed volumetric flow rate and aeration rate, whereas an increase in viscosity of fluid reduced the extent of coalescence. Besides, the size distribution of oil droplets in the cyclonic separator, pipe flow section and column flotation section were simulated in the flotation column using a special software. The simulation was compared with experimental data on the mean size of oil droplets.

Keywords: cyclonic-static micro bubble flotation column, coalescence, multi-flow pattern, oily wastewater

Introduction

An oil droplets size distribution strongly influences efficiency of separation technologies. Fine oil droplets cannot be removed efficiently due to their small size, low density, low velocity etc. A coalescence technology plays an important role in separation of oily wastewater. Coalescence of oil droplets can significantly improve the oil-water separation efficiency by enlarging the oil droplets diameter and changing the oil droplets distribution, after which it is then combined with the proper subsequent separation process. Since 1970s, the coalescence technology has been applied to the field of oil-water separation (Scott, et al., 2001). In 1981, the coalescence technology was first applied in Daqing Oilfield (China).

The coalescence technology involves coalescence of fine oil droplets through either physical or chemical methods to form larger particles to enhance droplets separation. The coalescence mechanism includes collision and wetting. In the wetting coalescence, the size of oil droplets increases by wetting, collision, interception and adhesion based on the coalescence medium (packing), while in the collision coalescence, the dispersed oil droplets are collided with each other, resulting in either two or more oil droplets forming one larger droplet. In recent years, the researches on the coalescence methodologies focused on coalescence mechanism (Boyson and Pashley, 2007; Mitre et al., 2010), packing (Wilkinson and Waldie, 1994; Dyakowski and Williams, 1996; Wang, 2003; Ni and He, 2007; Qu et al., 2009; Zhang et al., 2009), wetting (Hong et al., 2003; Ji et al., 2009), cyclone (Yeung et al., 2003; Yuan and Zhang, 2005; Jin et al., 2009; Schutz et al., 2009), coalescence flotation and efficiency improvement (Urbina-Villalba and Garcia-Sucre, 2001; Martula et al., 2003; Fredrick et al., 2010; Ata et al., 2011), gravity (Li and Gu, 2005; Sokolovic et al., 2007), electric field coalescence (Lee et al., 2001; Bresciani et al., 2010) and ultrasonic coalescence (Pandu and Donald, 2007; Pangu and Feke, 2009; Junji et al., 2009).

In the present study, in order to improve the separation efficiency of fine oil droplets from oily wastewater, a device named cyclone-static micro bubble flotation column by multi-flow pattern coalescence was developed. The cyclone-static micro bubble flotation column has been widely applied in mineral processing and wastewater treatment. For instance, a full-scale tests of 2000 m³/day using the cyclone-static micro bubble flotation column, which was constructed and operated at the Shengli Oilfield (China), oil removal of 97.70% with the treated effluent containing an oil concentration of 23.39 mg/dm³ was obtained (Li et al., 2015). The size distribution of oil droplets in the cyclonic separator for cyclonic coalescence, pipe flow section for pipe flow coalescence and flotation column for laminar flow coalescence were analyzed. The effects of process parameters such as circulation pressure, aeration rate, feed volumetric flow rate and viscosity of fluid on the efficiency of multi-flow pattern coalescence were investigated. The size distribution of oil droplets in the cyclonic separator, pipe flow section and flotation column were simulated in the flotation column using the Fluent software.

Coalescence phenomena in the cyclonic static micro-bubble flotation column

Coalescence occurs when either two or more oil droplets collide. The collision is caused by spatial velocity differences between droplets. During the oil-water separation process, droplets coalescence can increase the oil droplets size. It significantly improves the oil removal efficiency when combined with the subsequent separation process.

The cyclone-static micro bubble flotation column (Fig. 1) consists of three zones, that is flotation separation (upper section), cyclonic separation (lower section) as well as bubble generated and pipe flow zone (external section). The main components of the device are: flotation column, recycling pump and micro bubble generator (Liu, 1998; Li et al., 2015). The oily wastewater is pumped into the column through an inlet about one-quarter the way down from the top, and the treated water leaves the bottom of the column via the clean effluent discharge pipe, while the oil-laden foam overflows from the top of the foam discharge tank. The wastewater with poor floatability, containing very fine oil droplets, is split from the column, about three-quarters the way down from the top, and is tangentially pumped into the internal cyclone through the micro bubble generator and piping. Air is introduced into the generator and bubbles are produced. The fine oil droplets are loaded onto the bubbles and carried from the cyclonic separation zone to the flotation separation zone.
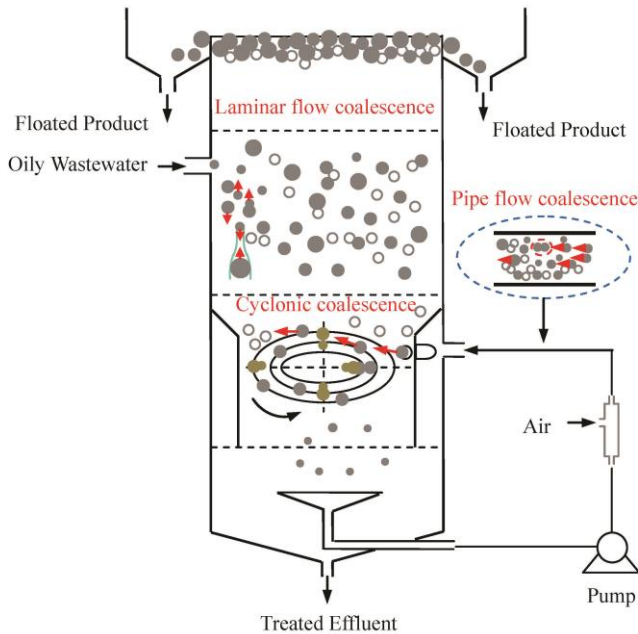

Fig. 1. Coalescence in the inner cyclonic separator of the flotation column

In the processing of separation by flotation, there are three kinds of coalescence processes such as cyclonic, pipe flow and laminar flow coalescence being revealed in the cyclonic-static micro bubble flotation column. As shown in Fig. 1, the cyclonic coalescence of the oil droplets generally occurs in the cyclonic separation zone, which is a kind of air-injected inner cyclonic separator. The pipe flow coalescence of the oil droplets occurs in the pipe flow zone of the flotation column. The laminar flow coalescence of oil droplets generally occurs in the flotation separation zone. In the

cyclonic coalescence, the rotational velocity of liquid in the inner layer is higher than that in the outer layer because of the velocity difference along the tangential direction which is caused by shearing stress between droplets or tangential velocity gradient in the cyclonic separator. It results in an occurrence where the droplet moving in the rotating inner layer can catch up with the droplet moving in the rotating outer layer, thus two droplets can collide and coalesce. At the same time, the motion trails of droplets with different sizes can be intersected because of the velocity difference along the radial direction which is caused by the different diameters of droplets in the cyclonic field. The velocity towards the center of the large droplet is higher than that of the small droplet, resulting in occurrence of coalescence between two droplets with different sizes. In the processing of pipe flow coalescence, coalescence is performed between the small droplets with high velocity and large droplets with low velocity in the same direction motion process. It results in occurrence of coalescence and formation of larger droplet. In the processing of laminar flow coalescence, coalescence occurs between the floated upward droplets and entrained downward droplets in the feed flow in the gravity field. It also results in coalescence and formation of larger droplet (Zhang and Yuan, 2003).

Experimental

Materials

A sample of crude oil used in this study was obtained from the Shengli Oilfield (China). The chemical composition of the sample used for preparation of 1 dm^3 oil-water emulsion with an oil concentration of 20,000 mg/dm^3 is as follows: crude oil 20 g, sodium petroleum sulfonate 5 g, sodium carbonate 10 g and sodium dodecylbenzenesulfonate 15 g. In order to obtain a stable oil-water emulsion, crude oil, sodium petroleum sulfonate, sodium carbonate, sodium dodecylbenzenesulfonate (SDBS, $C_{18}H_{29}NaO_3S$) were mixed at various speeds above 3000 rpm for 30 min at 60 ^{o}C so that the oil droplets were dispersed completely in water. The simulated samples were prepared by adding pre-determined amounts of the oil-water emulsion in a mixing tank and were emulsified by a static mixer and recycling through a pump for 90 min. The wastewater temperature was kept at 35-39 °C.

Equipment and methods

The experimental setup is shown in Fig. 2. The main device is a set of cyclonic-static micro bubble flotation column, which had 0.1 m diameter and 2 m height. A circulation pump with 0.5-1 m^3/h of discharge was used for the column. A flowmeter and a valve situated at the outlet of the circulation pump were used to measure and control the circulation volumetric flow rate. The oily wastewater was obtained by addition water in the mixing tank with a pre-determined amount of oil-water emulsion. The sampling points were shown in Fig. 2. The oil droplet size distribution was

analyzed with a laser particle analyzer (model BT-9300HT, Dandong Bettersize Instruments Ltd).
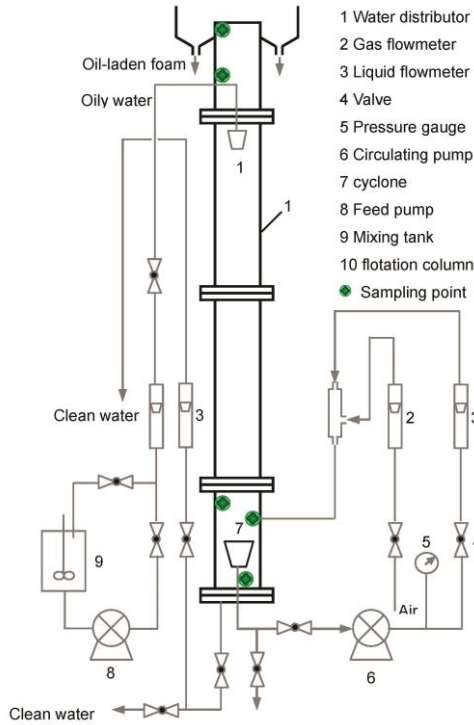

1 Water distributor
2 Gas flowmeter
3 Liquid flowmeter
4 Valve
5 Pressure gauge
6 Circulating pump
7 cyclone
8 Feed pump
9 Mixing tank
10 flotation column
● Sampling point

Fig. 2. Schematic of the cyclonic static micro-bubble
flotation column separation unit

Results and discussion

Multi-pattern coalescence

As shown is Figure 3, the mean diameter of the oil droplets increased with increasing the circulation pressure using multi-pattern coalescence. For example in the cyclonic coalescence, the mean size of droplets was 9.12 and 11.99 μm with an initial mean size of 6.56 and 7.96 μm, when the circulation pressure was 0.06 and 0.10 MPa, respectively. Furthermore, it appears that the increase amplitude of the mean size of droplets decreased slightly when the circulation pressure increased up to 0.12 MPa. It was also observed that the mean size of droplets was 7.96 μm after pipe flow coalescence, 11.99 μm after cyclonic coalescence and 23.66 μm after laminar flow coalescence with an initial mean size of 3.55 μm when the circulation pressures was 0.10 MPa. The circulation pressure was an important parameter in the flotation process of oily wastewater treatment when using a cyclone-static micro bubble

flotation column. There was the shearing force acting on the oil droplet, which caused oil droplet to deform, distort and break-up. Larger shear force acting on the oil droplet leads to distortion, deformation and break-up, while smaller shear force cannot produce coalescence caused by the velocity gradient. The cyclone becomes a coalescer when the coalescence plays a dominant role in the process, otherwise, the cyclone becomes an emulsifier.
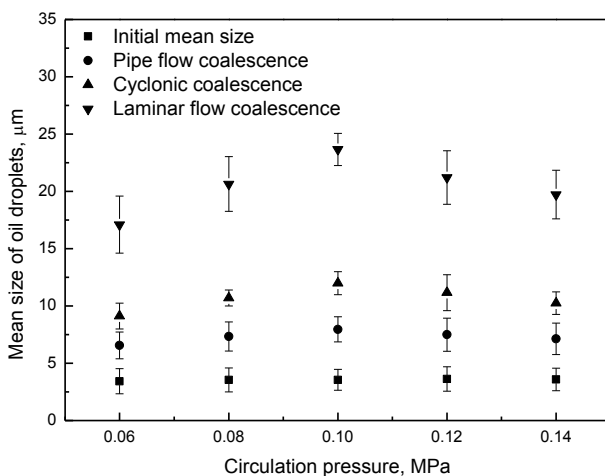

Fig. 3. Effect of circulation pressure on multi-pattern coalescence

As shown is Figure 4, the mean diameter of the oil droplets increased with increasing the aeration rate using multi-pattern coalescence. For example in the cyclonic coalescence, the mean size of droplets was 9.04 and 10.75 μm with an initial mean size of 2.51 and 2.34 μm when the aeration rate was 1.0 and 2.0 dm^3/min, respectively. Furthermore, it appears that the increase amplitude of the mean size of droplets decreased slightly when the aeration rate increased up to 2.0 dm^3/min. It was also observed that the mean size of droplets was 6.79 μm after pipe flow coalescence, 10.75 μm after cyclonic coalescence and 22.83 μm after laminar flow coalescence with an initial mean size of 2.34 μm when the aeration rate was 2.0 dm^3/min. In the cyclonic coalescence, the large aeration rate led to an amount of fine oil droplets entering column flotation section by entrainment of fluid in quasi forced vortex, while small aeration rate removed the droplets from the cyclone without collision and coalescence steps and form the "short circuit flow." In the laminar flow coalescence, the collision and coalescence probability between oil droplets decreased with increasing the aeration rate in the column flotation section. However, the fluid pattern changed when the aeration rate increased and the amount of fine oil droplets performed turbulent motion in the column flotation section, resulting in decrease of collision and coalescence.
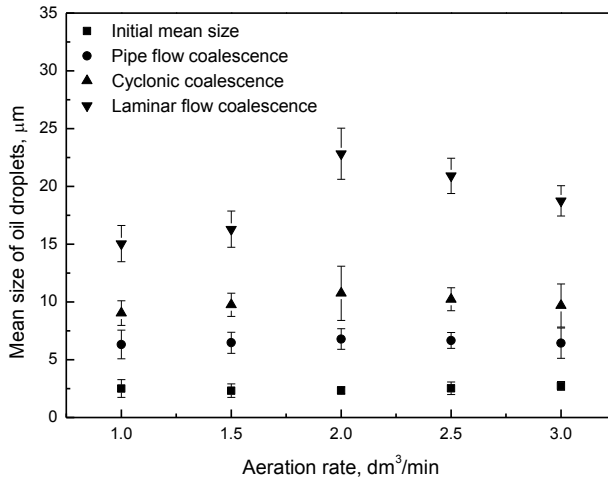
Fig. 4. Effect of aeration rate on multi-pattern coalescence

As shown is Figure 5, the coalescence ratio decreased with increasing the viscosity. For example in the cyclonic coalescence, the mean size of droplets was 11.21 and 8.26 μm with the initial mean size of 3.76 and 3.87 μm, when the aeration rate was 1.05 and 1.62 mPa·s, respectively. It was also observed that the mean size of droplets was 7.62 μm after pipe flow coalescence, 11.21 μm after cyclonic coalescence and 24.25 μm after laminar flow coalescence with an initial mean size of 3.76 μm when the viscosity was 1.05 mPa·s. The droplets moved slowly and the probability of mutual collision between droplets decreased when the viscosity was high. It resulted in decrease of the coalescence efficiency.
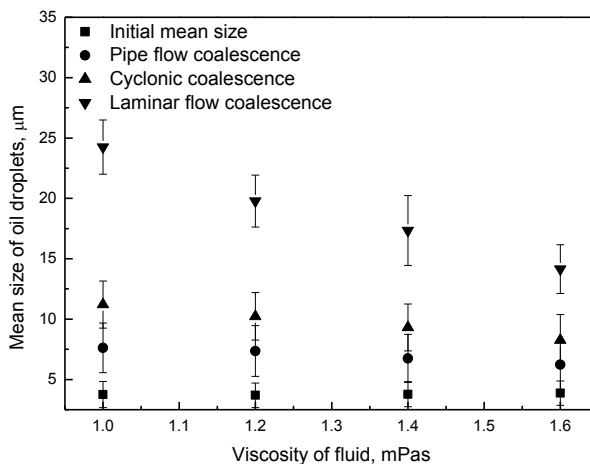

Fig. 5. Effect of viscosity of fluid on multi-pattern coalescence

Laminar flow coalescence

As shown in Figure 6, the coalescence efficiency increased with increasing the feed volumetric flow rate. The mean size of droplets was 25.03 μm after pipe flow coalescence with the initial mean size of 11.11 μm when the feed volumetric flow rate was 0.20 dm³/min. Furthermore, it appears that the increase amplitude of the mean size of droplets decreased slightly when the feed volumetric flow rate increased up to 0.25 dm³/min. The bubbles and oil droplets floated upward in the flotation column due to density difference. The floating velocity of oil droplets and bubbles followed the Stokes Law. The residence time in the flotation column was shortened when the feed volumetric flow rate was higher than the critical feed volumetric flow rate, resulting in a decrease of coalescence efficiency, especially for the fine oil droplets.
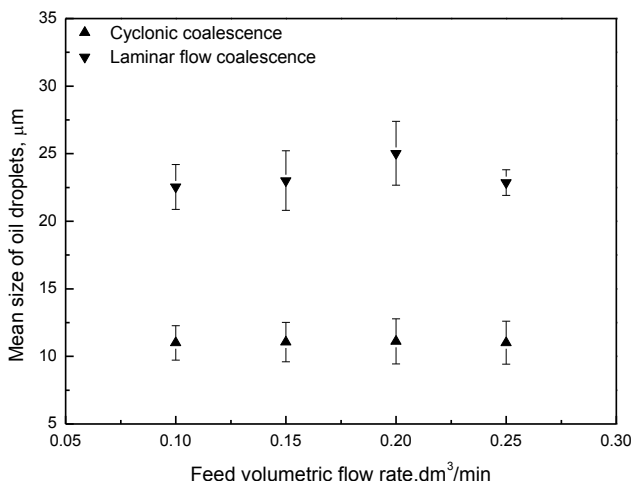

Fig. 6. Effect of feed volumetric flow rate on laminar flow coalescence

Effect of the coalescence efficiency on oil removal

In order to compare coalescence and process efficiencies between the cyclonic-static micro bubble flotation column and the conventional dissolved air flotation column, oily wastewater separation was carried out using two types of flotation columns. The dissolved air flotation column just performed laminar flow coalescence of the oil droplets without either the pipe flow coalescence or cyclonic coalescence in the flotation column. In this study, a set of dissolved air flotation column with 0.1 m diameter and 2 m height was used.

The oil removal efficiency of 93.49% was obtained with the treated wastewater effluent containing a final oil concentration of 30.48 mg/dm³ using the cyclonic-static micro bubble flotation column, while an oil removal efficiency was equal to 72.55% with a final oil concentration of 128.53 mg/dm³ using the dissolved air flotation column under conditions as following: a 0.20 dm³/min of feed volumetric flow rate,

2.0 dm^3/min of aeration rate, 1.12 mPa·s of viscosity of fluid, 0.1 MPa of circulation pressure, 468.25 mg/ dm^3 of initial oil concentration and 2.52 μm of mean oil droplet size in the feed. The mean oil droplet sizes were 20.69 and 13.75 μm at the cross section of the cyclonic-static micro bubble flotation column and the dissolved air flotation column, respectively. It shows that the cyclonic-static micro bubble flotation column is efficient for separation of fine oil droplets.

Flow field simulation of the multi-flow pattern coalescence

The flow field simulation of multi-flow pattern coalescence was developed with the commercial software Fluent 7.0 (Zhao et al., 2000; Wang, 2004). In order to solve the flow field simulation of multi-coalescence and the equation of motion of the dispersed phase, it was assumed that: (*i*) the oil/water medium is a liquid-liquid two-phase flow; (*ii*) it is an incompressible Newtonian fluid; (*iii*) the fluid temperature is constant, and (*iv*) the fluid model follows the corresponding control equation.

Two-phase flow model determination

In this work, the Eulerian model (Qian et al., 2011) was used to simulate the liquid-liquid two-phase flow field using Fluent 7.0. The Eulerian model is widely applied in simulation of the non-free liquid level two-phase flow. In the Eulerian equation, the effective density of q phase is $\hat{\rho}_q = \alpha_q \rho_q$.

The q phase continuity equation can be expressed as,

$$\frac{\partial}{\partial t}(\alpha_q \rho_q) + \nabla \cdot (\alpha_q \rho_q \vec{v}_q) = \sum_{p=1}^{n} \dot{m}_{pq} \tag{1}$$

where $\vec{v}_q$ is q phase speed; $\dot{m}_{pq}$ is the mass transfer between p phase and q phase.

The q phase momentum balance equation can be expressed as:

$$\frac{\partial}{\partial t}(\alpha_q \rho_q \vec{v}_q) + \nabla \cdot (\alpha_q \rho_q \vec{v}_q \vec{v}_q) = -\alpha_q \nabla p + \nabla \cdot \overline{\overline{\tau}}_q + \sum_{p=1}^{n} (\vec{R}_{pq} + \dot{m}_{pq} \vec{v}_{pq}) + \alpha_q \rho_q (\vec{F}_q + \vec{F}_{lift,q} + \vec{F}_{Vm,q}) \tag{2}$$

where $\overline{\overline{\tau}}_q$ is the pressure strain tensor of the q phase:

$$\overline{\overline{\tau}}_q = \alpha_q \mu_q (\nabla \vec{v}_q + \nabla \vec{v}_q^T) + \alpha_q (\lambda_q - \frac{2}{3}\mu_q) \nabla \bullet \vec{v}_q \overline{\overline{I}} \tag{3}$$

where μ_q, λ_q is the shearing viscosity and volume viscosity of q phase; $\vec{F}_q$ is the volume force; $\vec{F}_{lift,q}$ is the float force; $\vec{F}_{Vm,q}$ is the virtue mass force; $\vec{R}_{pq}$ is the interphase mutual acting force; p is the pressure, and $\vec{v}_{pq}$ is the interphase relative velocity.

Turbulence model

In order to solve the turbulence flow field, the Renault stress should be considered for the irregular pulse of fluid flow and some relevant equations should be used (Han et al., 2004; Wang et al., 2007).

The STD $k-\varepsilon$ turbulence model was used in the engineering program, k equation is the turbulence energy and ε is the turbulence energy dissipation rate. The simulated data is in accordance with the experiment data with smaller wall pressure gradient using the STD $k-\varepsilon$ model.

The turbulence energy equation (k equation) can be expressed as:

$$\frac{\partial}{\partial t}(\rho k) + \frac{\partial}{\partial x_i}(\rho k u_i) = \frac{\partial}{\partial x_j}\left[\left(\mu + \frac{\mu_t}{\sigma_k}\right)\frac{\partial k}{\partial x_j}\right] + G_k + G_b - \rho\varepsilon - Y_M + S_k \tag{4}$$

The energy dissipation equation (ε equation) can be expressed as:

$$\frac{\partial}{\partial t}(\rho\varepsilon) + \frac{\partial}{\partial x_i}(\rho\varepsilon u_i) = \frac{\partial}{\partial x_j}\left[\left(\mu + \frac{\mu_t}{\sigma_\varepsilon}\right)\frac{\partial\varepsilon}{\partial x_j}\right] + C_{1\varepsilon}\frac{\varepsilon}{k}(G_k + C_{3\varepsilon}G_b) - C_{2\varepsilon}\rho\frac{\varepsilon^2}{k} + S_\varepsilon \tag{5}$$

where G_k is the turbulence energy due to the speed gradient; G_b is the floating force due to the turbulence energy; Y_M is the fluctuation due to transient diffusion; $C_{1\varepsilon}$, $C_{2\varepsilon}$, $C_{3\varepsilon}$ is the constants; σ_k, σ_ε is the turbulence Prandtl number of k and ε equations; S_k, S_ε is the source phases (Wang et al., 2007); μ_t is the vortex viscosity coefficient.

The vortex viscosity is defined as:

$$\mu_t = \frac{C_\mu \rho k^2}{\varepsilon} \tag{6}$$

where C_μ is a constant.

The empirical relevant parameters using the STD $k-\varepsilon$ model were given as follows: $C_{1\varepsilon} = 1.44$, $C_{2\varepsilon} = 1.92$, $C_{3\varepsilon} = 0.09$, $\sigma_k = 1.0$ and $\sigma_\varepsilon = 1.3$.

Model geometry and boundary conditions

A schematic diagram of the flotation column for simulation is shown in Fig. 7. The model geometry (a 3D modeling) was structured using AutoCAD software and saved into a .sat file. The computational grid for flotation column (a hexahedral grid) was generated with the Gambit software containing 200,000 elements.

The model boundary type was also given when the grid was generated. The upper inlet was defined as the velocity inlet, the bottom treated effluent discharge was defined as the velocity outlet, and the cyclonic separator inlet was also defined as the velocity inlet. The initial oil concentration in feed was 0.05%. The simulation was

carried out under condition of continuous feed, floated oily foam and treated effluent discharge. The boundary conditions were defined as follows.
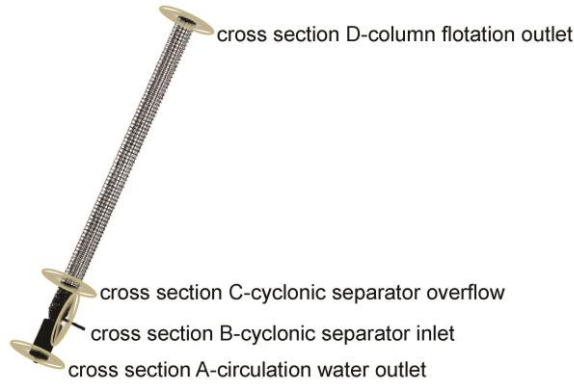

cross section D-column flotation outlet

cross section C-cyclonic separator overflow
cross section B-cyclonic separator inlet
cross section A-circulation water outlet

Fig. 7. Grid division of flotation column and test point position

1) For cyclonic separator inlet it was assumed that the oily wastewater entering into the cyclonic separator was uniformly mixed, and the inlet velocity and phase volume fractions of oily wastewater were given.
2) For the bottom treated effluent and circulating wastewater the outlet velocity was given according to the experimental data, the circulating wastewater outlet velocity was the same as the inlet velocity of cyclonic separator.
3) For the feed inlet the velocity was the same as the experimental data.
4) The walls were applied with the non-slip boundary condition.
   The simulation parameters are shown in Table 1.

Table1. Parameters used in simulation

Height of flotation column, mm	2000
Diameter of flotation column, mm	100
Feed velocity, m/s	2.45
Circulating water velocity, m/s	0.45
Treated effluent velocity, m/s	0.057
Initial oil concentration, %	0.20
Density of water phase, kg/m^3	998.20
Viscosity of water phase, mPa·s	1.003
Density of oil phase, kg/m^3	960.00
Viscosity of oil phase, mPa·s	48.00

Simulation results and analysis

In order to compare the simulation and experimental results, four cross sections were structured along the flotation column (Fig. 7). The size distribution of oil droplets and

mean size of these four cross sections are presented in Fig. 8. As shown in Fig. 8, the mean size of oil droplets at the cross section A in the bottom circulating wastewater was 1.32 μm. The mean size of the oil droplets at the cross section B was 5.24 μm before entering the inlet of cyclonic separator after performing the pipe flow coalescence. The mean size of oil droplets at the cross section C in the upper section of cyclonic separator was 10.20 μm after performing cyclonic coalescence. The mean size of oil droplets at the cross section D in the upper column flotation was 18.50 μm after performing laminar flow coalescence. The simulation results indicated that the mean size of oil droplets gradually increased after performing multi-flow pattern coalescence in the flotation column, and the simulation data was consistent with the experimental data in the aspect of gradually increasing trend by multi-flow pattern coalescence. However, the simulation data slightly underestimated the experimental data because of the experimental conditions and errors.
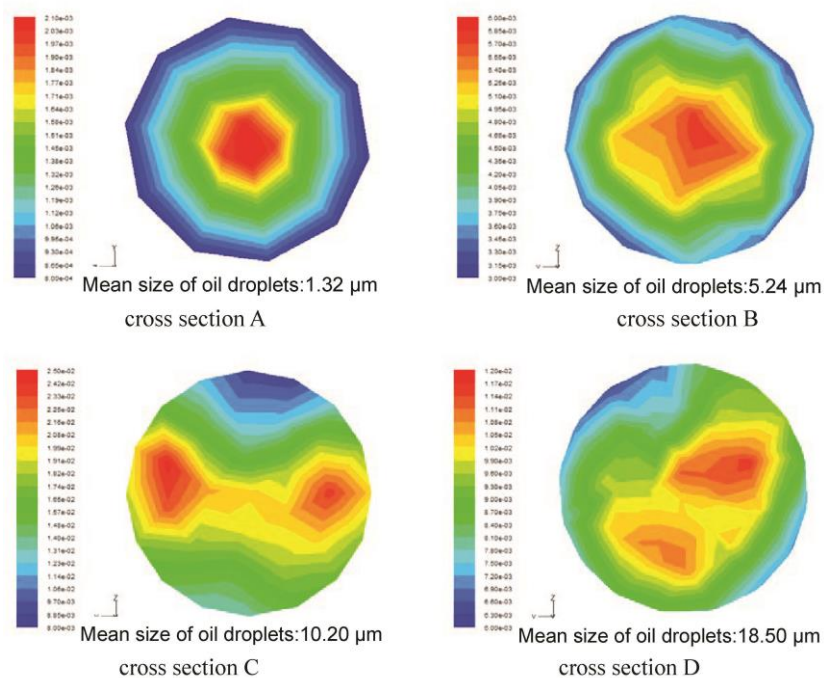

Fig. 8. The oil particle size distribution at each floatation column section

Conclusions

The cyclonic-static micro bubble flotation column was developed to separate oil/water by combining the hydraulic cyclonic separator with the conventional flotation column. Separation was integrated with flotation, cyclone and coalescence. The size of fine droplets was increased by multi-flow pattern coalescing in the flotation column. The

multi-flow pattern coalescence process was as follows: cyclonic coalescence in the inner cyclonic separator, pipe flow coalescence in the pipe flow mineralization zone, laminar flow coalescence in the column separation zone. The size distribution oil droplets in the cyclonic separator, pipe flow section and column flotation was obtained after the numerical simulation of two-phase field in the flotation column using the software Fluent 7.0. It was found that the simulation results match well the experimental data.

Acknowledgements

References

BRESCIANI A.E., MENDONCA C.F.X., ALVES R.M.B., MASCIMENTO C.A.O., 2010. *Modeling the kinetics of the coalescence of water droplets in crude oil emulsions subject to an electric field, with the cellular automata technique*. Comput. Chem. Eng. 34, 1962-1968.

ATA S., PUGH R.J., JAMESON G.J., 2011. *The influence of interfacial ageing and temperature on the coalescence of oil droplets in water*. Colloid and Surface A 374, 96-101.

BOYSON T.K., PASHLEY R.M., 2007. *A study of oil droplet coalescence*. J. Colloid Interf. Sci. 316, 59-65.

DYAKOWSKI T., WILLIAMS R A., 1996. *Prediction of high solids concentration regions within a hydrocyclone*. Power Technol. 87, 43-47.

FREDRICK E., WALSTRA P., DEWETTINCK K., 2010. *Factors governing partial coalescence in oil-in-water emulsions*. Adv. Colloid Interface Sci. 153, 30-42.

PAUNGU G.D., FEKE D.L., 2007. *Droplet transport and coalescence kinetics in emulsions subjected to acoustic fields*. Ultrasonics 46, 289-302.

URBINA-VILLALBA G., GARCIA-SUCRE M., 2001. *Influence of surfactant distribution on the stability of oil/water emulsions towards flocculation and coalescence*. Colloid. Surface A 190, 111-116.

HAN Z., WANG J., LAN X., 2004. *Fluent simulation examples and Application*. Beijing Institute of Technology press: Beijing, China.

HONG A., FANE A. G., BURFORD R., 2003. *Factors affecting membrane coalescence of stable oil-in-water emulsions*. J. Membrane Sci. 222, 19-39.

JI F., LI C., DONG X., 2009. *Separation of oil from oily wastewater by sorption and coalescence technique using ethanol grafted polyacrylonitrile*. J. Hazard. Mater. 164, 1346-1351.

JIN X., JIN Y., WANG J., SUN Z., CHEN X., 2009. *Separation performance of gas-liquid cyclone separator*. J. China Univ. Petroleum 33, 124-129.

JUNJI F., HARUKI T., NARUYA I., 2009. *Possibility of coalescence of water droplets in W/O emulsions by means of surface processes*. Colloid Surface A 333, 53-58.

LEE C.-M., SAMS G.W., WAGNER J.P., 2001. *Power consumption measurements for ac and pulsed dc for electrostatic coalescence of water-in-oil emulsions*. J. Electrostat. 53, 1-24.

LI J., GU Y., 2005. *Coalescence of oil-in-water emulsions in fibrous and granular beds*. Sep. Purif. Technol. 42, 1-13.

LIU J., 1998. *Study on cyclonic-static micro bubble flotation column and preparation technology of clean coal*, Ph.D. dissertation. China University of Mining and Technology, Beijing, China.

LI X., LIU J., WANG Y., XU H., CAO Y., DENG X., 2015. *Separation of oil from wastewater by coal adsorption-column flotation*. Sep. Sci. Technol. 50, 583-591.

MITRE J.F., TAKAHASHI R.S.M., RIBEIRO C.P., 2010. *Analysis of breakage and coalescence models for bubble columns*. Chem. Eng. Sci. 65, 6089-6100.

NI L., HE L., 2007. *Experimental studies of separating behavior of gravitational oil-water separator with a coalescing internal install*. Oil Field Equipment 36, 61-64.

PANGU G.D., FEKE D.L., 2009. *Kinetics of ultrasonically induced coalescence within oil/water emulsions: Modeling and experimental studies*. Chem. Eng. Sci. 64, 1445- 1454.

QIAN Z., HU X., HUAI W., XUE W., 2011. *Numerical simulation of sediment erosion by submerged jets using an Eulerian mode*. Sci. China: Technological Sciences, 41, 419-425.

QU X., NI L., LIU X., ZHU W., 2009. *Research on the factors of impacting the coalescence efficiency*. J. Filtr. Separat. 19, 14-16.

SOKOLOVIC R.M.S., VULIC T.J., SOKOLOVIC S.M., 2007. *Effect of bed length on steady-state coalescence of oil-in-water emulsion*. Sep. Purif. Technol. 56 , 79-84.

SCOTT K., JACHUCH R.J., HALL D., 2001. *Cross flow microfiltration of water-in-oil emulsion using corrugated membranes*. Sep. Purif. Technol. 11, 431-441.

SCHUTZ S., GORBACH G., PIESCHE M., 2009. *Modeling fluid behavior and droplet interactions during liquid–liquid separation in hydrocyclones*. Chem. Eng. Sci. 64, 3935-3952.

MARTULA S.D., BONNECAZE R.T., LLOYD D.R., 2003. *The effects of viscosity on coalescence-induced coalescence*. Int. J. Multiphas. Flow 29, 1265-1282.

WANG F., 2004. *Fluid dynamics analysis: Theory and application CFD software*. Tsinghua University press: Beijing, China.

WANG R., ZHANG K., WANG G., 2007. *Fluent technology and application*. Tsinghua University press: Beijing, China.

WANG Z., 2003. *Research on the structure and the characteristics of compound hydrocyclones*, Ph.D. dissertation. Harbin Engineering University, Harbin, China.

WILKINSON D., WALDIE B., 1994. *CFD and experimental studies of fluid and particle flow in horizontal primary separation*. Chem. Eng. Res. Des. 72, 189-196.

YEUNG A., MORAN K., MASLIYAH J., 2003. *Shear-induced coalescence of emulsified oil drops*. J. Colloid Interf. Sci. 265, 439-443.

YUAN H., ZHANG X., 2005. *Investigation into mechanism of coalescence in vortex field*. Chem. Eng. 33, 30-33.

ZHANG L., HE L., WANG T., LÜ Y., HE Z., 2009. *Separating behavior with coalescence internals in separator*. J. Chem. Eng. Chinese Univ. 23, 345-350.

ZHANG M., YUAN H., 2003. *Methods, mechanism and application of coalescence separation*. J. Filtr. Separat. 13, 44-46.

ZHAO X., SU M., ZHANG C. MIAO Y., 2000. *CFD techniques for design of fluid machinery*. Fluid Machinery 28, 22-25.